

# Experiment of FMCW Radar for Small Displacement Detection using VNA

Solihatul Jannah  
Dept. Electrical Engineering  
Telkom University  
Bandung, Indonesia

aatsolihatuljannah@student.telkomuni-  
versity.ac.id

Aloysius Adya Pramudita  
Dept. Electrical Engineering  
Telkom University  
Bandung, Indonesia

pramuditaadya@telkomuniversity.ac.id

Fiky Y Suratman  
Dept. Electrical Engineering  
Telkom University  
Bandung, Indonesia

fysuratman@telkomuniversity.ac.id

**Abstract**—Small displacement detection is indispensable for the monitoring process in several fields such as the health of large building structures, landslides, monitoring of vibrations in large mechanical structures, and also in the health sector. Non-contact monitoring processes will provide an advantage in covering a large area operation. The radar system is potentially applied as a noncontact sensor. However, small displacement detection requires high resolution referring to the range resolution perspective. Detecting a small displacement on a millimeter to centimeter scale requires a very wide bandwidth. The main information to be obtained from small displacement detection is the distance of the target and the size of the small displacement. Frequency modulation continuous wave (FMCW) is a radar system that has been widely used in various fields. In this paper, a small displacement detection method is proposed by developing the detection capabilities of the FMCW radar. The ability to detect distance using beat frequency identification is maintained and phase detection is elaborated to detect small displacement without having to increase bandwidth. The experimental modeling of proposed FMCW using a vector network analyzer (VNA) was conducted in this study. The results show that the proposed FMCW system using VNA has the ability to detect small displacement with average phase shift of 0.41 radians for a 2 mm shift in the direction close to the target and 0.44 radians for the direction away from the target.

**Keywords**—small displacement, radar, FMCW, and VNA.

## I. INTRODUCTION

Small displacement has become a concern in several fields. For example, in various studies, monitoring methods for small displacement have been studied in several studies such as health monitoring of building structures [1-2], landslides [3-4], and in the medical field such as respiration and heart rate monitoring [5-6]. In the several previous cases, the small displacement scale is in the order of millimeters to centimeters. In some previous cases of small displacement detection, it is also necessary to cover a large area or cover many observation points.

Radar is a system used to detect information from targets such as location, movement, size, or other information using the concept of electromagnetic wave propagation [7]. The use of a radar system as a non-contact scanning method is a solution in the case of small displacement detection. The use of a radar system has the potential to monitor a large area without having to use many sensors [8]. The application of a radar system as a non-contact sensor in the medical, such as detecting human respiration or heart rate provide better comfort, hygiene [9-12], and allows multi target detection. The radar system has also begun to be studied for detecting the displacement in large building structures such as large bridges or high-rise buildings. The displacement that occurs

in the structure then becomes an indicator of health condition of the structure.

Frequency modulation continuous wave (FMCW) radar systems have been widely applied for various needs [13-17]. A number of experiments using the FMCW system have been carried out including detecting small shifts modeled on each trihedral reflecting object mounted at a number of positions on the structure [18-20]. The FMCW system principle in detecting the distance using the beat frequency can be supported the radar capability in multi-target detection.

The deficiency of the FMCW system in detecting small displacements by using beat frequencies then becomes a problem that motivates the elaboration of phase detection in the proposed method. Small displacement detection requires high resolution and from a distance resolution perspective, the bandwidth of the radar signal must be extensively large for obtaining the millimeter to centimeter scale resolution. The ability of the FMCW system to detect the target position is maintained in the proposed method. The ability to detect distance can be used to determine to differentiate several targets, and allowing the radar system to cover a wide observation area. Modification of the FMCW radar system by adding a phase detection process as proposed in [17], then elaborated as a small displacement detection technique in the proposed method. In this study, experimental analysis was carried out by modeling the FMCW radar using vector network analyzer (VNA)

This paper was organized as follows: In section II, the proposed method for detecting small displacements is explained. Then section III describes the experimental scheme carried out in this study and the experimental results and analysis are discussed in section IV. Finally, the conclusion is in section V.

## II. FMCW RADAR SYSTEM FOR SMALL DISPLACEMENT DETECTION

The FMCW radar is a continuous radar which using, periodic linear functions such as saw-tooth signals for modulating the sinusoidal radar signal [7]. The FMCW radar system consists of voltage control oscillator as a signal generator which is controlled by a saw-tooth signal. The signal is then passed through the splitter to the power amplifier and mixer. After being amplified, the signal is transmitted through the transmitting antenna. The reflected signal from the target received by the antenna will then be amplified by the low noise amplifier (LNA) and then sent to the mixer. The mixer output will be filtered using low pass filter (LPF). The use of LPF aims to get a beat signal that is used to detect the target distance. Fast Fourier transform (FFT) calculation is applied

to identify the beat frequency value which is then used to determine the target distance. The in-phase and quadrature (IQ) demodulator was added to the computation/software part to calculate the phase of the beat signal. The output of the IQ demodulator is the result of small displacement detection. The proposed FMCW system can be seen in Fig. 1 and the radar system illustration in detecting the small displacement is depicted in Fig. 2.

To overcome the problem of small displacement detection resolution on the conventional FMCW radar, then the proposed method elaborates the phase data processing and applying for the LPF output of mixer. The phase processing using an IQ demodulator is added as post processing part of the FMCW radar system. As shown in Fig. 2,  $T_x$  is the transmitted signal,  $R_x$  is the received signal,  $d_0$  is the distance from the radar to the target, and  $d_t$  is the small displacement. The LPF output frequencies for  $d_0$  and  $d_0 + d_t$  is quite the same because  $d_0 + d_t \approx d_0$ . When the system bandwidth is not reached the resolution requirement, then the results of the beat frequency detection cannot be used to identify  $d_t$ . Then the small displacement  $d_t$  is obtained by performing phase detection of the LPF output signal. The LPF output can then be written in (1).

$$S_{LPF}(t) = A_m \cos(2\pi f_0 \Delta_t) + A_m \cos\left(2\pi \frac{\Delta_f \Delta_t}{T} t\right) \quad (1)$$

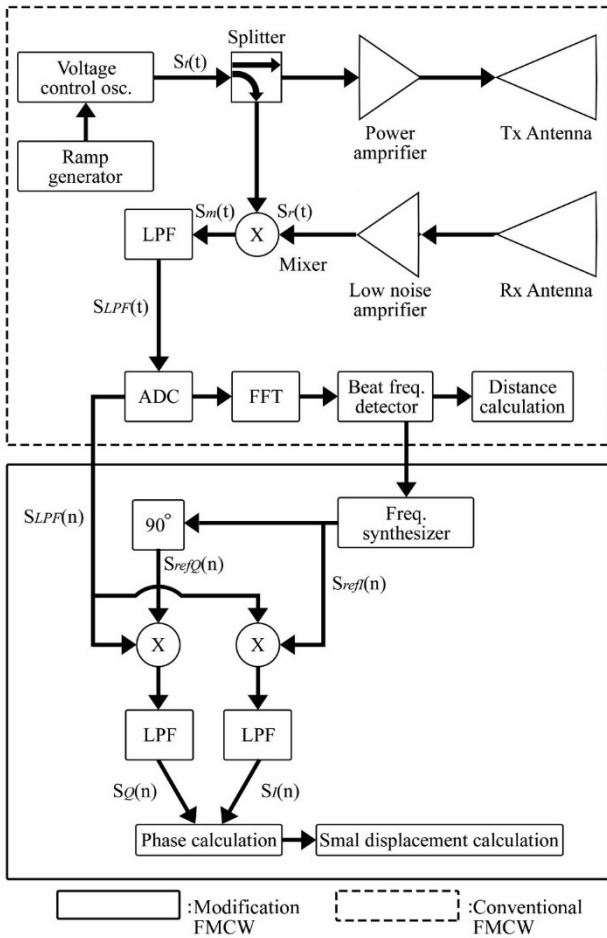


Fig. 1. Proposed improvements to the FMCW radar system for small displacement detection.

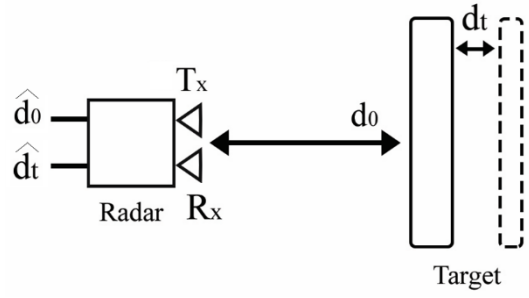


Fig. 2. Radar for small displacement detection.

$$\Delta_t = \frac{2(d_0 + d_t)}{v_p} \quad (2)$$

Where  $A_m$  is the amplitude,  $f_0$  is the frequency,  $\Delta_f$  is the bandwidth of the FMCW signal,  $\Delta_t$  is the propagation delay that can be written as (2),  $T$  is the chirp period of the FMCW signal,  $t$  is the time,  $v_p$  is the propagation speed of the radar wave. The reference sinusoidal signal used in the IQ demodulator computation is then divided into two components, the first is the reference signal for the in-phase arm and the second is the reference signal for the quadrature arm. Both of references signals are written as (3) and (4).

$$S_{refI}(t) = A_0 \cos\left(2\pi \frac{\Delta_f \Delta_t}{T} t\right) \quad (3)$$

$$S_{refQ}(t) = A_0 \sin\left(2\pi \frac{\Delta_f \Delta_t}{T} t\right) \quad (4)$$

The mixer output on the in-phase and quadrature arms can then be written as (5) and (6). To get the phase component from the displacement, the high frequency component from the mixer output is eliminated by using the LPF. The LPF outputs in the in-phase and quadrature arms shown by (7) and (8), respectively. The phase detection result is then obtained by using the arcus tangent calculation as in (9).

$$S_{mI}(t) = A_m \left[ \cos\left(2\pi f_0 \Delta_t + 4\pi \frac{\Delta_f \Delta_t}{T} t\right) + \cos(2\pi f_0 \Delta_t) \right] \quad (5)$$

$$S_{mQ}(t) = A_m \left[ \sin\left(2\pi f_0 \Delta_t + 4\pi \frac{\Delta_f \Delta_t}{T} t\right) + \sin(2\pi f_0 \Delta_t) \right] \quad (6)$$

$$S_I(t) = A_m [\cos(2\pi f_0 \Delta_t)] \quad (7)$$

$$S_Q(t) = A_m [\sin(2\pi f_0 \Delta_t)] \quad (8)$$

$$\Delta_t = \tan^{-1} \left( \frac{S_Q(t)}{S_I(t)} \right) \quad (9)$$

The FFT calculation for the  $S_{LPF}$  signal is used to estimate the beat frequency and then can be used to determine the target distance  $d_0$ . Furthermore, by substituting (9) to (2) and using the  $d_0$  value that has been obtained, the  $d_t$  value can then be obtained. Small displacement can be detected

properly when the small displacement that occurs is less than a quarter of the wavelength at the lowest frequency of the chirp signal used. When the small displacement size is greater than a quarter of a wavelength, the periodic phase repetition of a sinusoidal signal exhibits the ambiguity of the detected phase data.

For example, in detecting the human respiration using a radar system, the small displacement that occurred in the chest or abdominal wall during breath is time-varying. Therefore, the output of the phase detection is also time-varying and representing the pattern of the chest or abdominal wall during breathing.

### III. FMCW MODEL USING VNA EXPERIMENT

VNA is a measuring instrument used to measure the scattering parameters of a N port network or system. The advantage of VNA is the ability to measure the complex quantities. Traditional test equipment such as power meters, spectrum analyzers, and oscilloscopes usually only have a received signal magnitude. In contrast, VNA has a source and a set of receivers that are used to determine the stimulus change induced by device under test (DUT). The stimulus-based test approach allows the VNA to measure very small reflections and changes to the stimulus allowing it to accurately characterize any RF component in real-world environments and testing conditions.

The concept of the FMCW radar modeling in the laboratory experiment is determined considering the physical meaning of  $S_{21}$  measurement using VNA. The setup of radar modeling using VNA is depicted in Fig. 3. The two VNA ports are then connected to the antenna, the measured  $S_{21}$  data can be associated to the transfer function between the received and transmitted signals. In modeling the FMCW radar, therefore the transmitted signal is the FMCW signal that is generated on the transmitter side. In this study, the transmitted signal  $S_t(t)$  is a chirp signal with a certain period and bandwidth. Furthermore, the received signal can be determined using relation that written in (10) and (11) [21].

$$S_r(f) = S_{21}S_t(f) \quad (10)$$

$$S_r(t) = F^{-1}[S_r(f)] \quad (11)$$

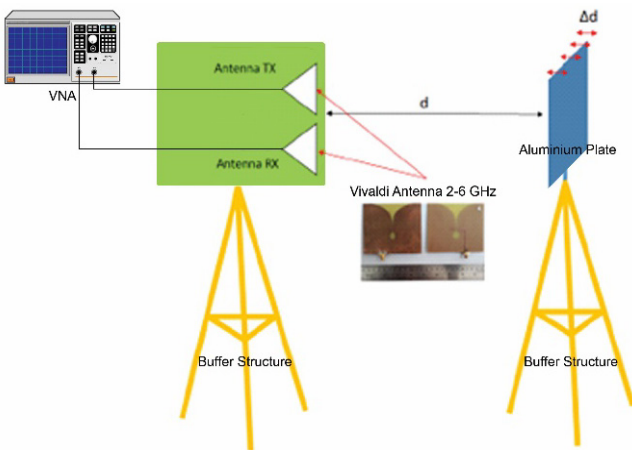


Fig. 3. Experimental model with VNA.

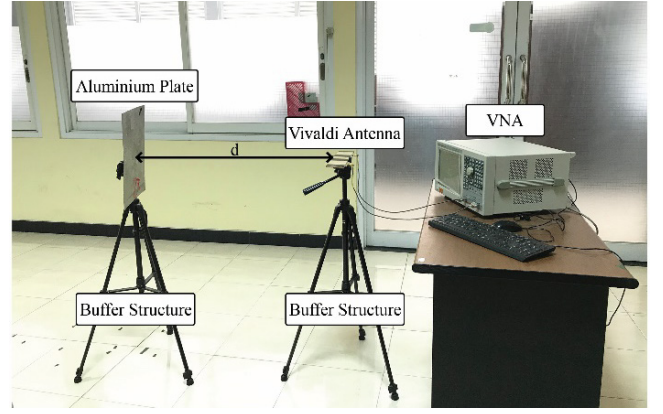


Fig. 4. Measurement scenarios using VNA with objects.

$$S_t = A_t \cos \left[ 2\pi \left( f_0 + \frac{4f}{T} t \right) t \right] \quad (12)$$

$S_r$  is to receive signal,  $S_t$  is the FMCW signal as written in (12), and  $F^{-1}$  is the inverse Fourier transform. The experimental model of FMCW radar for small displacement using VNA is depicted in Fig. 3.

VNA is used as transmitter and receiver and the measurement output of the VNA that is used is  $S_{21}$  data. The Vivaldi antenna is connected to the VNA on port 1 and port 2. Port 1 represents a transmitter and port 2 as a receiver.  $d$  is the distance from the antenna to the target. The aluminum plate is used as a target, that is placed in front of the radar at a specified distance. The computation steps that employed to the  $S_{21}$  data that discussed in [21] is used to obtain the received signal. The computation for obtaining the received signal form measured  $S_{21}$  was performed in the laptop that receiving the measurement data from VNA. The experimental model that has been carried out using the VNA is shown in Fig. 4.

### IV. RESULT AND DISCUSSION

The experiment was carried out aimed at obtaining detection results in the form of the target distance ( $d_0$ ) and the small displacement that occurred at the target ( $d_t$ ). The first step is to observe the ability of the proposed radar system to work at 2 GHz with a bandwidth of 200 MHz, and chirp period of 30  $\mu$ s to detect the target distance. Experiments were carried out at three different distances, namely 100 cm, 150 cm, and 200 cm. In the experiment, the measurement data were processed using Matlab software. Beat frequency detection results are shown in Fig. 5.

In Fig. 5, the blue line depicts the measurement results in conditions without a target. It appears that the frequency spectrum of the LPF output has a low value, therefore it can be used as a baseline that indicate there is no significant beat frequency that is identified associated with a target. The red line represents the measurement results with a targeted distance of 100 cm. The output of the LPF has a peak spectrum at a frequency of 5.4 MHz and it can be concluded that the beat frequency is located at 5.4 MHz. The yellow line depicts the measurement results with a targeted distance of 150 cm. The LPF output has a peak of 6.6 MHz and it can be concluded that the beat frequency is located at 6.6 MHz. The purple line represents the measurement result with a target distance of 200 cm. The LPF output has a peak of 8.4 MHz

and it can be concluded that the beat frequency is located at 8.4 MHz. Based on the detected beat frequency, the targets at three different distances can be detected as having different beat frequencies. With a bandwidth of 200 MHz, the FMCW system has a distance resolution of 75 cm, so that for a target distance of 100 cm and 200 cm the difference in beat frequency position is clearer compared to distance of 100 cm and 150 cm. Based on the results obtained, it can be concluded that the FMCW and VNA radar system modeling can work well and show its ability to detect target distances. Experiments were carried out several times to ensure that the results obtained were consistent.

The second step is to make small displacement at the target with several values of 2 mm, 0.5 cm, and 1 cm. Fig. 6 and Fig. 7 show the results of beat frequency detection with a 2 mm shift toward the radar and step away from the radar.

In Fig. 6, the LPF output shows when the target distance is 99.2 cm due to a small displacement of 2 mm toward the radar. Where as in Fig. 7, the LPF output shows when the target distance is 100.2 cm due to a small displacement of 2 mm step away from the radar. From the figure, it can be seen that the locations of the beat frequency values are coincided and it is difficult to distinguish for two different positions as far as 2 mm. Based on these results it can be concluded that a small displacement of 2 mm cannot be detected using beat frequency data. In Fig. 8 shows the detected beat frequency respecting several positions around 1 m distance from the radar. It can be seen from the result that the small distance difference in millimeter scale is difficult to identify from the change of beat frequency.

The third step is to perform the phase detection processing with IQ demodulator for obtaining small displacement data that cannot be obtained using beat frequency. In the experiment, a small displacement was carried out on the target with a scale of 2 mm. Fig. 9 is a graph of the phase detector output as a result of small displacement detection with a 2 mm shift toward the radar. The graph depicts the phase change as the target shifts every 2 mm closer to the radar. The average phase detector output for a small displacement approaching the radar is 0.41 radians. Based on the graph, it can be concluded that each small displacement results in a different phase output. For a shift closer to the radar, the phase detector output tends to increase. Fig. 10 is a graph of the phase

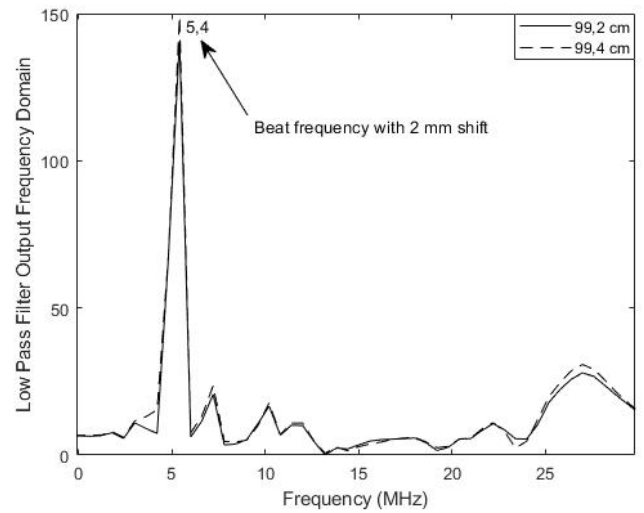


Fig. 6. Frequency spectrum of LPF output for target at a distance of 100 cm and a small displacement of 2 mm occurs toward the radar.

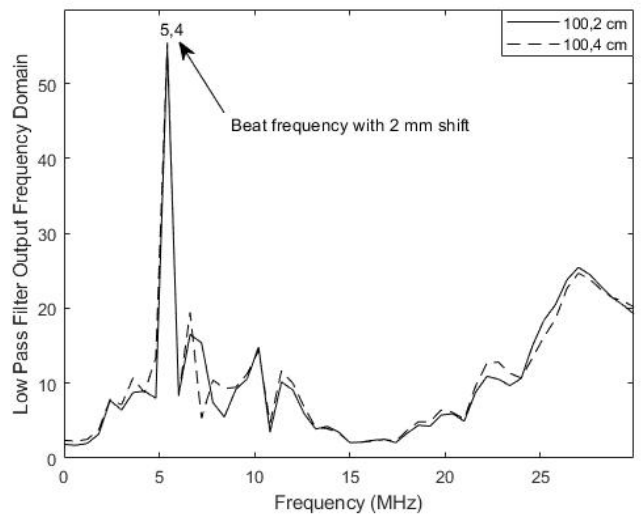


Fig. 7. Frequency spectrum of LPF output for target at a distance of 100 cm, a small displacement of 2 mm occurs step away from the radar.

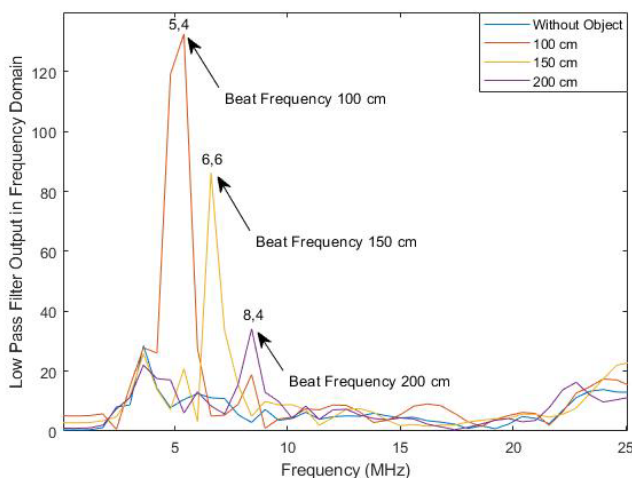


Fig. 5. Beat frequency for the target at several different distance from the radar.

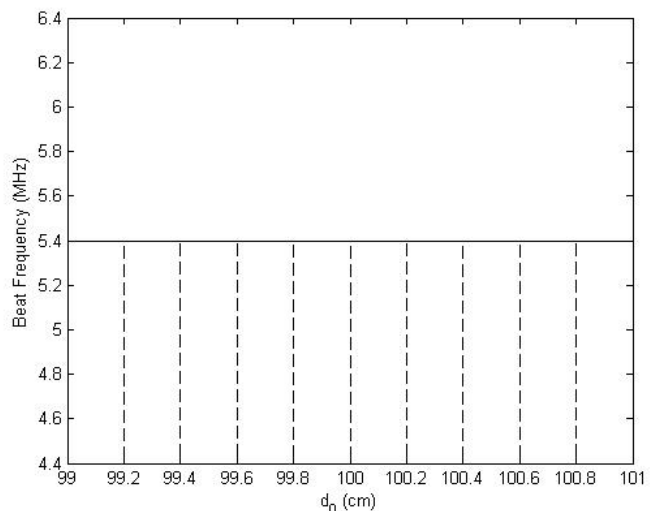


Fig. 8. Beat frequency detection results for small displacement.

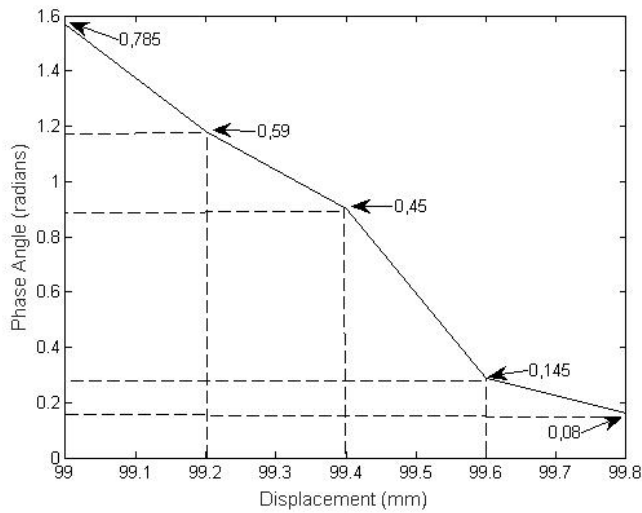


Fig. 9. Output phase detector for small displacement 2 mm approaching radar.

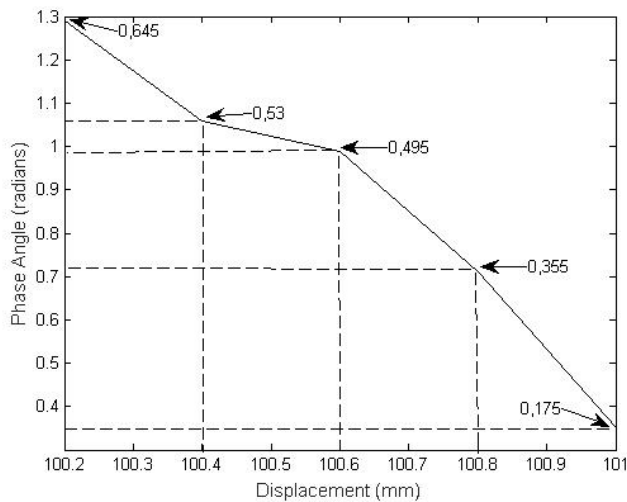


Fig. 10. Output phase detector for small displacement 2 mm away from radar.

detector output as a result of small displacement detection with a 2 mm shift away from the radar. The graph depicts the phase change as the target shifts every 2 mm away from the radar. The average phase detector output for small displacement away from the radar is 0.44 radians. Based on the graph, it can be concluded that each small shift results in a different phase output. For a shift away from the radar, the phase detector output tends to increase. But in theoretically, the change in the phase detector output value for the small displacement per 2 mm is linear. However, the result in Fig. 9 and Fig. 10, the graph shows the phase detection output which is not exactly linear. This can be caused by the influence of noise or interference that may appear when making measurements in the laboratory room. When the phase detector is employed for small displacement detection, therefore the detection capability is limited by the repetition of phase value every multiple of wavelength. Respecting to the frequency that used in the experiment 2 GHz, therefore the small displacement ambiguity is 15 cm.

## V. CONCLUSION

The modeling of the FMCW radar system using a VNA device to detect a small displacements has been carried out. The detection result consists of distance detection and the value of small displacement that occurred on the target. The beat frequency detection of the FMCW radar signal is maintained to determine the target distance and the phase detection of the beat signal using the IQ demodulator is used to determine the small displacement that occurs on the target. The results of FMCW radar modeling using VNA show that the model can represent the FMCW system. The results of beat frequency detection show the target distance can be distinguished based on the beat frequency value. The results also show that the small displacement that occurs in the target can be detected based on the output of the phase detector. For shifts toward the radar, the output of the phase detector tends to increase, while for shifts away from the radar, the output of the phase detector tends to decrease. The results show that the proposed FMCW system using VNA has the ability to detect small displacement with average phase shift of 0.41 radians for a 2 mm shift in the direction close to the target and 0.44 radians for the direction away from the target.

## REFERENCES

- [1] M. R. Kaloop, E. Elbeltagi, J. W. Hu and A. Elrefai, "Recent advances of structures monitoring and evaluation using GPS-Time series monitoring systems: A review," *Int. J. Geo-Information* 2017, vol. 6, no. 12, p. 382, Nov. 2017, doi: 10.3390/IJGI6120382.
- [2] J. J. Lee and M. Shinozuka, "A vision-based system for remote sensing of bridge displacement," *Nondestructive Testing and Evaluation Int.*, vol. 39, no. 5, pp. 425-431, Jul. 2006, doi: 10.1016/J.NDTEINT.2005.12.003.
- [3] D. Zhang, M. Kurata and T. Inaba, "Small displacement detection of biological signals using the cyclic frequency method," *Int. J. Antennas Propag.*, vol. 2015, 2015, doi: 10.1155/2015/842123.
- [4] C. C. Chung and C. P. Lin, "A comprehensive framework of TDR landslide monitoring and early warning substantiated by field examples," *Eng. Geol.*, vol. 262, Nov. 2019, doi: 10.1016/J.ENGGEOL.2019.105330.
- [5] C. Zhong, Y. Liu, P. Gao, W. Chen, H. Li, Y. Hou, T. Nuremanguli and H. Ma, "Landslide mapping with remote sensing: Challenges and opportunities," *Int. J. Remote Sensing*, vol. 41, no. 4, pp. 1555-1581, Feb. 2019, doi: 10.1080/01431161.2019.1672904.
- [6] M. Arima, H. Araki and Y. Iwamoto, "Feasibility study of measuring heartbeat and respiration by using strain gauge," in *7th Int. Conf. Emerging Trends Eng. Technol.*, Sakai, Japan, 2015, pp. 147-152, doi: 10.1109/ICETET.2015.24.
- [7] M. Skolnik, *Radar Handbook*, 3<sup>rd</sup> Ed., America: McGraw-Hill Education, 2008.
- [8] F. Liang, F. Qi, Q. An, H. Lv, F. Chen, Z. Li and J. Wang, "Detection of multiple stationary humans using UWB MIMO radar," *Sensors*, vol. 16, no. 11, Nov. 2016, doi: 10.3390/S16111922.
- [9] S. Pisa, E. Pittella, and E. Piuze, "A survey of radar systems for medical applications," *IEEE Aerosp. Electron. Syst. Mag.*, vol. 31, no. 11, pp. 64-81, Nov. 2016, doi: 10.1109/MAES.2016.140167.
- [10] R. Ambarani, A. A. Pramudita, E. Ali and A. D. Setiawan, "Single Tone doppler radar system for human respiratory monitoring," in *2018 5th Int. Conf. Electrical Engineering, Computer Science and Informatics*, Malang, Indonesia, 2018, pp. 571-575, doi: 10.1109/EECSI.2018.8752871.
- [11] S. Jannah, A. A. Pramudita and Y. Wahyu, "Self-complementary bowtie antenna design for UWB respiration," in *2019 Int. Conf. Information and Communications Technology*, Yogyakarta, Indonesia, Jul. 2019, pp. 237-242, doi: 10.1109/ICOIAC.2019.8938450.
- [12] K. A. C. de Macedo, F. L. G. Ramos, C. Gaboardi, J. R. Moreira, F. Vissirini and M. S. d. Costa, "A compact ground-based interferometric radar for landslide monitoring: the xerém experiment," *IEEE J. Sel. Top. Appl. Earth Obs. Remote Sens.*, vol. 10, no. 3, pp. 975-986, Mar. 2017, doi: 10.1109/JSTARS.2016.2640316.



- [13] C. Li, W. Chen, G. Liu, R. Yan, H. Xu and Y. Qi, "A noncontact FMCW radar sensor for displacement measurement in structural health monitoring," *Sensors*, vol. 15, no. 4, pp. 7412-7433, Mar. 2015, doi: 10.3390/S150407412.
- [14] D. Zhang, M. Kurata and T. Inaba, "FMCW radar for small displacement detection of vital signal using projection matrix method," *Int. J. Antennas Propag.*, vol. 2013, 2013, doi: 10.1155/2013/571986.
- [15] M. Alizadeh, G. Shaker and S. Safavi-Naeini, "Experimental study on the phase analysis of FMCW radar for vital signs detection," in *2019 13th European Conf. Antennas and Propagation*, Canada, 2019.
- [16] S. Kashyap, J. Stanier, A. Louie, S. Mishra and C. Larose, "RCS of a trihedral corner reflector," in *Symp Antenna Technology and Applied Electromagnetics*, Canada, 1994.
- [17] A. A. Pramudita, F. Y. Suratman, D. Arseno and E. Ali, "FMCW radar post processing method for small displacement detection," in *Proc. 2018 IEEE Int. Conf. Aerospace Electronics and Remote Sensing Technology*, Bali, Indonesia, 2018, pp. 61–65, doi: 10.1109/ICARES.2018.8547073.
- [18] Y. Qin, D. Perissin and L. Lei, "The design and experiments on corner reflectors for urban ground deformation monitoring in Hongkong," *Int. J. Antennas Propag.*, vol. 2013, 2013, doi: 10.1155/2013/191685.
- [19] K. Sarabandi and T. C. Chiu, "Optimum corner reflectors design," in *Proc. 1996 IEEE National Radar Conf.*, USA, 1996, pp. 148–153, doi: 10.1109/NRC.1996.510672.
- [20] A. G. Stove, "Modern FMCW radar - techniques and applications," in *First European Radar Conf. 2004*, Amsterdam, Netherlands, 2004.
- [21] A. A. Pramudita, T. O. Praktika and S. Jannah, "Radar modeling experiment using vector network analyzer," in *2020 Int. Symp. Antenna and Propagation*, Osaka, Japan, 2021, pp. 99–100, doi: 10.23919/ISAP47053.2021.9391495.